Confining the motion of enzymes in nanofiltration membrane for efficient and stable removal of micropollutants

Zhang, Hao; Luo, Jianquan; Woodley, John M.; Wan, Yinhua

Published in:
Chemical Engineering Journal

Link to article, DOI:
10.1016/j.cej.2020.127870

Publication date:
2021

Document Version
Peer reviewed version

Confining the motion of enzymes in nanofiltration membrane for efficient and stable removal of micropollutants

Hao Zhang [a], *Jianquan Luo* [a,*], *John M. Woodley* [b], *Yinhua Wan* [a]

[a] State Key Laboratory of Biochemical Engineering, Institute of Process Engineering, University of Chinese Academy of Sciences, Chinese Academy of Sciences, Beijing 100190, China

[b] Department of Chemical and Biochemical Engineering, Technical University of Denmark, 2800, Kgs. Lyngby, Denmark

* Corresponding author: E-mail: jqluo@ipe.ac.cn (J. Luo)

Abstract

Enzymes in living cells are highly dynamic but at the same time regularly confined for achieving efficient metabolism. Inspired by this phenomenon, we have prepared a novel biocatalytic membrane with high enzyme activity and stability by tuning the confinement strength of the membrane to enzyme, which was achieved via modifying the support layer of a polymeric nanofiltration (NF) membrane and reversely filtrating enzyme. A mussel-inspired coating was used to modify the support interior of the NF membrane to enhance charge and steric effects on enzyme, thus stabilizing enzyme in the membrane with little increment in mass transfer resistance for substrate and products (only 20% permeability loss with a high enzyme loading of 1.34 mg/cm^2). A suitable confinement strength of the membrane to enzyme could delayed the enzyme leakage and endowed enzyme with certain mobility for efficient reaction. Thus, the obtained biocatalytic membrane exhibited a negligible decline in BPA removal efficiency for 7 reuse cycles (less than 3.5%) or 36 hours continuous operation (less than 1%) in flow through mode, resulting in a long-term stability adequate for micropollutant removal. For the first time, enzyme mobility was defined and calculated to quantify the confinement strength of the membrane, which could be used to optimize the microenvironment for enzyme immobilization and predict the performance of the biocatalytic membrane. This work concluded that rationally regulating the enzyme mobility in the membrane and a periodic back-flushing operation for redistribution of enzymes could achieve a long-term stable removal of micropollutant in water by a biocatalytic membrane.

Keywords: micropollutants, biocatalytic membrane, enzyme mobility, enzyme immobilization, confinement strength

1 Introduction

Micropollutants such as endocrine disrupters, pesticides, pharmaceutical and personal care products result in detrimental effects on public health and aquatic ecosystems [1]. Moreover, the complicated physicochemical properties and the very low concentration of the micropollutants in water make them difficult to remove [2, 3]. Enzymes are green and sustainable catalysts with remarkable catalytic properties for treating micropollutants which have attracted increasing attention [4]. However, their poor stability and difficulties in recovery still limit their potential for widespread industrial application [5]. Hence, enzyme immobilization as a cost-effective method to improve enzyme stability and recyclability has been highly researched in the last decades [6]. Various carriers such as magnetic nanoparticles [7], metal-organic frameworks (MOFs) [8], mesoporous silica [9], and microspheres [10] have been developed for enzyme immobilization, however it is still a conundrum to meet the demands of real applications. By the virtue of good biocompatibility, low-cost, and easy functionalization with materials of interest, membrane is considered as a promising carrier for enzyme immobilization [11-13]. It not only ameliorates stability and reusability of free enzyme, but also endows the membrane with catalytic function, thereby greatly diminishing membrane fouling and adsorption saturation caused by micropollutants [14-16]. In addition, compared with the regular diffusion-controlled biocatalytic processes, the biocatalytic membranes can be operated in flow through mode (convective transport) which efficiently accelerates the mass transfer of the substrates and facilitates *in-situ* product removal, thus elevating enzyme activity, as well as avoiding the products inhibition on the immobilized enzymes [17, 18]. As a consequence, the integration of membrane separation and enzyme catalysis is a win-win strategy that exhibits a bright application prospect.

The functionalized polymeric and ceramic microfiltration/ultrafiltration (MF/UF) membranes have been widely used to immobilize enzymes, exhibiting high enzyme loading,

and low permeation resistance [19-22]. However, MF/UF membranes cannot reject micropollutants leading to a high catalytic burden on enzymes [20], and the polymerized hydrophobic products and other unfavorable foulants tend to adsorb in the membrane pores, thus resulting in serious membrane fouling and enzyme inactivation [21]. Enzyme has also been immobilized on the surface of the modified nanofiltration (NF) membrane, however, the enzyme loading is low due to the small specific surface area and limited active cites, and the immobilized enzyme is exposed to the accumulated foulants, leading to an inferior catalytic performance [23, 24]. To solve the above problems, immobilizing enzyme in the support layer of NF membrane is promising as the large specific surface area of the support layer endows the biocatalytic membrane with a high enzyme loading [25]. Moreover, the skin layer (thickness <1 μm and pore size < 2 nm) of the NF membrane can selectively shield the enzyme from unfavorable components and reject a part of micropollutants prior to being catalyzed by the immobilized enzyme, which maintains the stable enzyme catalytic microenvironment, reduces enzyme catalytic burden, and contributes to high micropollutants removal efficiency [26, 27]. Nevertheless, the support layer with large and gradient pore size cannot well retain the enzyme, thus the immobilized enzyme would be washed out when the biocatalytic membrane is operated in flow through mode (skin layer facing feed) [28, 29]. In order to prevent enzyme leakage, polydopamine (PDA) coating was used to seal enzyme inside NF membrane, and nanomaterials (e.g. graphene oxide and metal organic frameworks) were embedded into the support layer to adsorb and stabilize enzyme [26, 27, 30, 31]. Despite the high enzyme loading and low leakage, enzyme is immobilized in an extremely constrained environment with an inflexible structure resulting in low enzyme activity. Moreover, the high steric hindrance around the enzyme inhibited the access of the substrate and the leaving of the products, thereby further reducing the enzyme activity and stability.

Inspired by the fluid mosaic model of the cell membrane structure, we can know that the mobility of membrane protein embedded in the confined matrix of phospholipid is significant for its stability and enzymatic activity [32, 33]. Therefore, a desirable enzyme immobilization strategy needs to establish a balance between enzyme mobility and leakage. As we known, polyelectrolytes possess excellent conformational flexibility, chain mobility, electrostatic interaction and negligibly spatial diffusion limitation, which can effectively prevent enzyme agglomeration and possibly promote the catalytic performance of the immobilized enzyme [34-36]. For instance, polyethyleneimine (PEI) is a water-soluble cationic polymer which has gained enormous attention in drug carrier systems for proteins and peptides [37]. Its high hydrophilicity, inherent positive charge, and facile functionalization properties are conductive to construct an optimal microenvironment for immobilizing enzymes [38]. Hence, the modification of the support layer via PEI grafting may regulate the enzyme mobility in the NF membrane by increasing the steric and charge effects on enzyme, which is promising to minimize enzyme leakage and endow the immobilized enzyme with requisite mobility.

Laccase, a multi-copper oxidase enzyme, which can efficiently catalyze the oxidation of phenolic compounds such as bisphenol A (BPA) and chlorophenols, was widely chosen for preparing biocatalytic membrane [39]. However, the poor stability of laccase at 25°C (half-life of <1day) restricts its industrial application [40]. Herein, we have embedded enzyme into NF membrane by a facile and mild strategy, and the synergistic effect of membrane separation and enzyme catalysis results in a high removal efficiency of micropollutants. The great improvement has been made in enhancing the long-term stability and high catalytic activity of the biocatalytic membrane by tuning the confinement strength of the support layer to laccase. First, PEI was applied to modify the whole support layer of NF membrane (termed three-dimensional (3D) modification), to enhance the confinement strength of the membrane to enzyme. Laccase was subsequently noncovalently restricted in a modified NF membrane by

reverse filtration without sealing operation or insertion of nanomaterials (Figure 1). The properties of the prepared biocatalytic membranes (enzyme distribution, enzyme loading, storage stability) were evaluated and then the universality of such enzyme immobilization strategy was explored using other enzymes. After that, the micropollutant removal efficiency under flow through and static contact modes were compared, and the reusability and stability of the biocatalytic membrane in long-term operations were examined. In addition, for the first time, a simple protocol was used to quantify the mobility of the immobilized enzyme in the membrane. The quantitative enzyme mobility was proposed to reflect the confinement strength of the porous supports, as well as the catalytic performance of the immobilized enzymes. The outcome of this work would not only offer a novel biocatalytic membrane preparation strategy, but also provide a new direction to design an optimal confinement environment for enzyme immobilization.

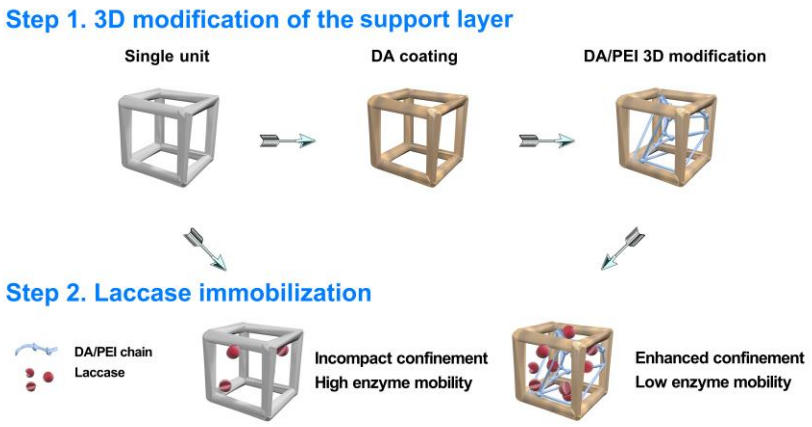

Figure 1. Schematic illustration of the 3D modification of the membrane support layer and corresponding enzyme immobilization.

2 Experimental section

2.1 Materials

NF270 membrane (molecular weight cut off (MWCO) ≈ 200-300 Da) was purchased from DOW-FILMTEC Co. (USA), which consists of a polyamide skin layer and a UF membrane

support with a polysulfone layer and a non-woven fabric layer. A dead-end filtration cell (Millipore, USA) with an effective area of 13.4 cm^2 was used to prepare the biocatalytic membranes and test their performance. Tris(hydroxymethyl)ainomethane, PEI (10000Da), sodium chloroacetate, and 2,6-dimethoxy phenol (DMP) as substrate for laccase activity assay were supplied by Aladdin. Zinc sulphate heptahydrate and sodium dihydrogen phosphate dihydrate were purchased from Xilong Chemical Co., (Guangdong, China). BPA (96%) was purchased from J&K Chemical (Beijing, China). Acetic acid, hydrochloric acid, and ethanol were supplied by Beijing Chemical works (Beijing, China). Sodium acetate was purchased from Sinopharm Chemical Regent. Laccase (EC 1.10.3.2, 60-70 kDa, 0.53U mg^{-1}) from *Trametes versicolor*, Bradford regent used for protein assay, and dopamine hydrochloride were purchased from Sigma-Aldrich (Shanghai, China). Fluorescein isothiocyanate (FITC) and rhodamine b (RhB) were purchased from MedChemExpress Co., Ltd. (Shanghai, China). All the chemical reagents used in the experiments were of analytic grade.

2.2 Preparation and characterisation of 3D modified membrane

2.2.1 Preparation of PDA/PEI modified membrane

The pristine NF270 membrane was soaked in 50% ethanol for 10 seconds and then immersed in deionized water over night to remove protective agent. After that, the membrane was washed by NaOH solutions (pH=10) under flow-through mode for 20 mins at 2 bar and then the initial permeability of the membrane was tested with deionized water at 2 bar. After pretreatment, the membrane was placed on the dead-end filtration cell in reverse mode (own support layer facing feed with an extra polypropylene support between the skin layer and the membrane holder). As shown in Figure S1, first, dopamine solution (10 mL, 2 g L^{-1} in Tris buffer (50 mM, 25℃, pH=8.8)) was poured into cell with an agitation of 100 rpm for 2h forming a PDA adhesion layer on the inner surface of the support layer. Then long-chain PEI

polymer (10 mL, 2 g L^{-1} in pure water, 25℃) was added into the cell and grafted on the adhesion layer via Schiff-based and Michael addition reactions for 4 h to carry out 3D modification [41]. The hydrodynamic radius was approximately around 2 nm for 10000Da PEI chain [42] which was feasible to diffuse into the support layer of the NF membrane since the smallest pores in the support layer were larger than 2 nm (Figure S2). The fabricated PDA/PEI modified membrane was washed by deionized water for 30 mins and its water permeability was tested at 2 bar, and it was then moved to a beaker with deionized water and shaken for several hours to remove weakly bound PEI. The covalently linked PEI in the membrane was stable during continuous filtration at least 12 h without detectable leakage according to total organic carbon (TOC) analyser (Figure S3).

2.2.2 Preparation of Zn modified membrane

Zinc ions were further introduced into the PDA/PEI modified membrane as they could effectively immobilize laccase by coordination with the imidazole and thiol groups of laccases and serve as activators for increasing the activity of laccase[20]. Briefly, the prepared PDA/PEI modified membrane was further soaked in a sodium chloroacetate solution (20 mL, 40 mg mL^{-1} in a pH=12 NaOH solution) and shaken at 150 rpm for 12 h at 60℃ to form iminodiacetic acid (IDA) groups. After that, Zn^{2+} coupling was carried out by soaking the membrane in a $ZnSO_4$ solution (20 ml, 0.4M in deionized water, 60 ℃) for 12 h and shaken at 150 rpm. Here, the coupled zinc ions aimed at capturing enzyme by affinity interactions. Finally, the Zn^{2+} modified membrane was washed with deionized water for several hours to remove unbound Zn^{2+}.

2.2.3 Characterisation of 3D modified membrane

X-ray photoelectron spectroscopic (XPS, Thermoescalab 250Xi, Thermo Fisher Scientific Co., USA) element analysis with monochromatic Al-Kα X-ray source (hv=1486.6 eV) was

used to confirm the successful modification of the membrane. Zeta potential of the support layer of the pristine and PDA/PEI-modified membranes as a function of pH was measured by the SurPASS Anton Paar analyser. The desired pH (3-10) of the KCl (1mM) solution was adjusted with HCl and NaOH solutions. The contact angle of the support layer was tested by using a water drop shape system (OCA20, Dataphysics, Germany). The method for determining the pore size distribution was the same as our previous work [43].

2.2.4 Membrane water permeability

The permeability (L_p) of the membranes before and after modification was measured by deionized water, which can be summarized in Eq. 1.

$$L_p = \frac{V_p}{t \cdot A_m \cdot TMP}$$

here, V_p is the permeate volume after a certain time, A_m is the effective filtration area (13.4 cm^2) and TMP is the transmembrane pressure.

2.3 Preparation and characterisation of biocatalytic membrane

2.3.1 Preparation

The pristine, PDA/PEI-modified, and Zn^{2+}-modified membranes were first placed in the dead-end filtration cell under reverse mode. Then acetic binding buffer (pH=5, 10mM) was used to equilibrate the membranes for 20 mins at 2 bar. After that, 45 mL laccase solution (0.5 g L^{-1} in acetic buffer, 25℃, pH=5, 100 rpm) was added into the cell and reversely filtrated into the support layer of the pristine, PDA/PEI-modified, and Zn^{2+}-modified membranes, respectively, at 2 bar until 43 mL permeate was collected for enzyme loading analysis. Then 10 mL acetic buffer (pH=5,10mM) was added into the cell to wash the enzyme-loaded

membrane at 2 bar. 2 mL retentate and 10 mL washing residual were collected together for enzyme loading analysis. The obtained biocatalytic membranes were then washed with acetic buffer (20 mL, 2 bar, pH=5) in normal mode (skin layer facing feed) to remove the weekly adsorbed laccase. This washing solution (20 mL) was collected for enzyme loading analysis. After washing, the biocatalytic membranes were soaked in acetic buffer (20 mL, 10 mM, pH=5) at 4℃ overnight. Finally, the laccase-loaded membranes were put in the cell under normal mode, and 10 mL acetic buffer was used to wash the membranes again at 2 bar. The soaking and washing solutions (total 30 mL) were mixed and collected for analysis. The prepared biocatalytic membranes were respectively termed as Pristine-E, PEI-E and Zn-E. Their water permeability was also tested and calculated by Eq. 1.

2.3.2 Laccase distribution in the NF membrane

The FITC-labelled laccase was immobilized in the pristine, PDA/PEI-modified, and Zn^{2+}-modified membranes with the same method described in Section 2.3.1. The obtained membranes were used to analyse the enzyme distribution by CLSM on a Leica SP8 STED 3X system (Germany). The FITC-labelled laccase was prepared by the following procedures. Laccase solution (5 mg mL^{-1}) was first dissolved in carbonate buffer (50 mM, pH 9.0) which was prepared by mixing NaCl (7.36 g), Na_2CO_3 (1.06 g) and $NaHCO_3$ (7.56 g) into deionized water (1 L). FITC (1 mg mL^{-1}) solution was prepared with dimethyl sulfoxide. Then FITC solution was added dropwise into laccase (5 mg mL^{-1}) solution, and the mixed solution was then stirred at 4 ºC for 4 h. Afterward, NH_4Cl aqueous solution (2 mL, 50 mM) was added into the mixed solution to stop the reaction. Finally, the solution was dialyzed in phosphate buffer (50 mM, pH 7) for 48 h at 4 ºC to remove excess FITC.

2.3.3 Activity assay on skin and support layers of biocatalytic membrane

The catalytic activity on skin and support layers of the biocatalytic membranes was determined by recording the oxidation rate of DMP. The membranes were firstly put into the dead-end filtration cell in normal mode, and subsequently DMP solution (20 mL, 10 mM) prepared by acetic buffer (10 mM, pH=5) was poured into the cell to react for 4.5 mins with 100 rpm agitation. The change in absorbance at 468 nm was recoded every 0.75 min by a spectrophotometer. 1 mL solution was taken out each time and poured back to the cell after the test. One unit of laccase activity (U) was defined as the amount of laccase required to catalyse the conversion of 1 μmol DMP per minute at the above conditions. The activity of the biocatalytic membranes was calculated as unit per membrane area (U/m^2) according to Eq. 2.

$$\text{Enzyme Activity } (U/m^2) = \frac{Abs_{min} \cdot 10^6 \cdot V_t}{\varepsilon_{468} \cdot m \cdot A_m} \quad (2)$$

where, Abs_{min} is the absorbance per minute which is obtained from the slope of the initial linear portion of the kinetic curve (absorbance vs time), V_t is the volume of reaction system (L), ε_{468} is the DMP molar absorption coefficient ($\varepsilon_{468} = 49600\ (M \cdot cm)^{-1}$), m is the amount of the immobilized laccase (g), A_m is membrane surface area (0.00134 m^2).

The membranes were then washed with acetic buffer (10ml, 10 mM, pH=5) and put into the dead-end filtration cell in reverse mode. The same method was used to test the enzyme activity on the support layer.

2.3.4 Enzyme loading efficiency

Bradford method was used to measure the protein concentration of the samples [44]. The sample (1 mL) which was taken from enzyme solution was mixed with 1 mL Bradford assay. After 5 mins, the absorbance at 595 nm was recorded. The detection limit of protein with this

method was 20 μg L^{-1}. According to the mass balance, the amount of immobilized protein can be calculated as

$$M_{IMM} = C_f \cdot V_f - C_p \cdot V_p - C_R \cdot V_R - C_W \cdot V_W - C_{SW} \cdot V_{SW} \quad (3)$$

where M_{IMM} is the amount of immobilized protein, C_f, C_p, C_R, C_W, C_{SW} are the protein concentrations in the feed, permeate, retentate and washing residual, washing solutions in normal mode, and the mixture of soaking and washing solution, respectively. $V_f, V_p, V_R, V_W, V_{SW}$ are the volumes of the feed (45 ml), permeate (43 ml), retentate and washing residual (12 ml), washing solutions in normal mode (20 ml), and the mixture of soaking and washing solution (30 ml), respectively. The loading efficiency is expressed as Eq. 4.

$$\text{Loading efficiency} = \frac{M_{IMM}}{C_f \cdot V_f} \times 100\% \quad (4)$$

2.3.5 Storage stability of biocatalytic membrane

The biocatalytic membranes were stored in acetic buffer (20 mL, 10 mM, pH=5) at 4 ℃ for 7 days, and their catalytic activity was determined every day. The activity of the membranes was determined as described in Section 2.3.3. The initial activity was defined as 100%.

2.4 Enzyme immobilization mechanism of PEI-E

In order to analyse the contributions of steric and charge effects to laccase immobilization, a concentrated NaCl solution (1M) for shielding the charge effect was flowed through the membrane at 2 bar [45]. The permeate was collected every 5 mL and the released protein amount was tested. The washing step was stopped until no protein was detected.

2.5 Immobilization of different enzymes

Another four enzymes including glucose oxide (160 kDa), horseradish peroxidase (44 kDa), sucrase (270 kDa), and pepsin (35 kDa) were chosen as they have different molecular weights and isoelectric points. The charges and sizes of these enzyme are tested by Dynamic Light Scatter (DLS). The enzyme immobilization method was the same as mentioned in Section 2.3.

2.6 BPA removal by biocatalytic membranes

The catalytic performance of the biocatalytic membranes was evaluated by the biodegradation of a representative micropollutant BPA which has detrimental effects on human health even at trace levels. BPA solution used in this study was prepared by acetic buffer (10mM, pH=5.0) with a concentration of 10 mg L^{-1}.

2.6.1 BPA removal in static contact and flow through modes

In addition to Pristine-E, PEI-E and Zn-E, another biocatalytic membrane with sealing layer was prepared for comparison (termed as E-Sealing). Briefly, after reversely filtrating laccase solution into the pristine NF membrane, 10 ml Tris-HCl buffer (50 mM, pH 8.8) containing dopamine (2 g L^{-1}) and PEI (2 g L^{-1}) was added into the filtration cell and stirred at 100 rpm for 0.5 h to form a sealing layer. After that, the membrane was cleaned by deionized water and then soaked in 10 mL acetic buffer before use.

Four biocatalytic membranes were evaluated based on BPA removal efficiency in static contact and flow through modes, respectively. For contact mode, the membranes were soaked in 30 mL BPA solution for 3 h. After that, 4 mL solution was taken out and mixed with 2ml HCl solution (0.2 M) to terminate the enzymatic reaction. While for flow through mode, a BPA solution (33 mL) was added into the cell for filtration, where the permeate flux kept constant

at 7.46 L m^{-2} h^{-1} by manually controlling the operating pressure. Permeate (30 mL) was collected and mixed with HCl solution (15 mL, 0.2M) to terminate the enzymatic reaction.

The contribution of membrane adsorption and rejection to the BPA removal was assessed by an inactivated biocatalytic membrane. Such membrane was prepared by filtrating inactivated laccase, which was boiled until no activity was tested. The BPA removal efficiency (X_{BPA}) can be derived by Eq. 5.

$$X_{BPA} = (1 - \frac{C_p}{C_f}) \times 100\% \quad (5)$$

where, C_p and C_f are the concentrations of BPA in permeate and feed, respectively. BPA concentration in the samples was quantified by high performance chromatography (HPLC) (Shimadzu Co. Japan). HPLC was installed with two pumps, a UV-visible detector, an automatic sampler, a column oven and a C18 HPLC column (ZORBAX SB-C18, 250 mm×4.6 mm i.d.; 5 μm; Agilent, USA). HPLC analytic conditions are set as follows: isocratic elution with 50% ultrapure water and 50% HPLC-grade acetonitrile (V/V); flow rate of mobile phase is 1 mL min^{-1}; injection volume of the sample is 50 μL; the column oven temperature is set at 40℃; samples were detected at 278 nm and one sample took 15 min. The BPA retention time was around 5.98 min. The BPA detection limit in HPLC is 10 μg L^{-1}.

The specific catalytic efficiency of biocatalytic membrane for BPA removal was derived by Eq. 6.

$$\text{Specific catalytic efficiency} = \frac{X_{BPA,catalysis} \cdot C_p \cdot V_p}{100 \cdot m_{protein}} \quad (6)$$

where, $X_{BPA,catalysis}$ is the BPA removal efficiency by enzymatic catalysis and C_p is the concentrations of BPA in the feed. V_p is the volume of the permeate, $m_{protein}$ is protein amount of the immobilized laccase.

2.6.2 Reusability

The reusability of the biocatalytic membranes was evaluated by testing BPA removal efficiency for 7 reuse cycles in flow through mode. After each experiment, the membranes were washed with acetic buffer (10 mM, pH=5) under stirring (300 rpm) in an open cell for 20 min and then in flow through mode for 10 mins to remove the absorbed BPA and its products on/in the membrane. Finally, they were soaked in acetic buffer (10 mM, pH=5) at 4℃ overnight.

2.6.3 Long-term continuous operation

For continuous operation, an enzymatic membrane reactor with free laccase (same amount as the immobilized one) and a pristine NF270 membrane was constructed for comparison with pristine-E, PEI-E, Zn-E. BPA solution (10 mg mL^{-1}, pH=5.0) was continuously added into the cell and filtrated through the membranes at a constant permeate flux of 7.46 L m^{-2} h^{-1}. The permeate was collected after a few hours and mixed with HCl solution (0.2M) to terminate the enzymatic reaction. The BPA concentration in the collected samples was quantified by HPLC.

2.7 Tuning the confinement strength of the membrane

The different confinement strength of the NF membranes can be obtained by controlling the degree of PEI grafting in the support layer, which was achieved by changing the PEI grafting time. Therefore, the PEI grafting time was set at 0.1, 0.5, 2, 3, and 4 h respectively, and subsequently the same amount of laccase was filtered in reverse mode (termed as 0.1PEI-E, 0.5PEI-E, 2PEI-E, 3PEI-E and 4PEI-E).

2.8 Laccase motion in the membrane

Two methods were used to confirm the motion of laccase in the PEI-E. The first method was direct visualization of the laccase motion in the NF membrane via CLSM by washing the

biocatalytic membranes under reverse and normal modes in turn. The modified NF membrane was labelled with FTIC (green emission) and laccase was stamped with rhodamine b (Rhb, red emission). The second method employed the changes in the ratio of enzyme activity on skin and support layers to indirectly reflect the motion of laccase in the NF membrane. Theoretically, the ratio of enzyme activity on skin and support layers can represent the enzyme distribution in the NF membrane, and by washing the biocatalytic membrane in reverse or normal mode, the confined motion of laccase can be expressed by corresponding changes of the enzyme activity ratio. Hence, the PEI-E was successively washed in reverse, then normal and again reverse modes with acetic buffer (pH 5) at a permeate flux of 45.66 L m^{-2} h^{-1} for 12 h and the corresponding ratio of enzyme activity on skin and support layers was determined. Enzyme mobility can be calculated according to Eq.7:

$$\text{Enzyme mobility} = \frac{\alpha_f - \alpha_i}{\alpha_i} \times 100\% \quad (7)$$

where α_f and α_i are the final and initial ratios of the enzyme activity on skin and support layers, respectively.

2.9 Enzyme storage and controllable sustained-release device

Most of the prepared biocatalytic membranes showed excellent storage stability with negligible enzyme leakage, however, the immobilized enzyme would be finally washed out when operated at flow through mode. This gave the opportunity to use these membranes as a protein storage and sustained-release device. The protein release speed can be controlled by turning the confinement strength of the NF membrane to enzyme. Here two membranes including Zn-E and 2PEI-E were explored to release laccase under flow through mode at a permeate flux of 45.66 L m^{-2} h^{-1}. The permeate was collected every 30 mins and the amount of released laccase was determined by Bradford method.

3 Results and discussion

3.1 Characterization of 3D modified NF membrane

Successful modification of the support layer was confirmed by XPS analysis of the support layers of the pristine, PDA/PEI-modified and Zn-modified membranes (Table 1). It was obvious that the atomic fraction of N element increased after the PEI/PDA modification and element Zn appeared after Zn coupling. The appearance of the skin and support layers of the pristine and PDA/PEI-modified membranes was respectively shown in Figure S4. Different from the white color of the pristine membrane, the color of both sides of the PDA/PEI-modified membrane became dark brown, also verifying the membrane modification.

Table 1. XPS composition analysis on the support layers of pristine, PDA/PEI-modified and Zn-modified NF membranes

Elements	Atomic fraction [wt%]		
	Pristine	PDA/PEI modified	Zn modified
C	73.42	71.34	70.05
N	0.90	11.00	8.77
O	25.68	17.66	19.89
Zn	0	0	1.29
Total		100.00	

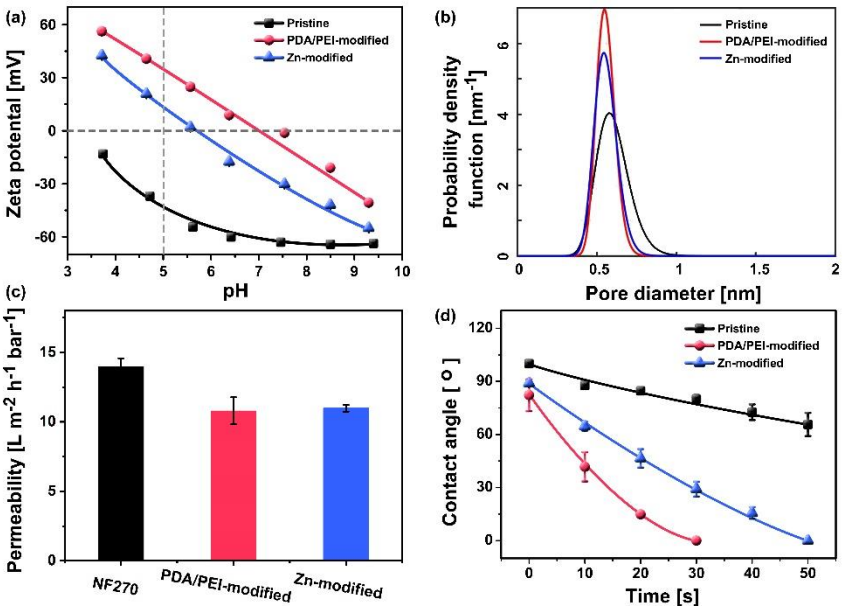

Figure 2. (a) Zeta potential on support layers; (b) membrane pore size distribution and (c) permeability; (d) contact angle of support layers of the pristine, PDA/PEI-modified and Zn-modified membranes. The error bars represent the standard deviation of at least three measurements.

Zeta potential on the support layers of the pristine, PDA/PEI-modified and Zn-modified membranes was shown in Figure 2a. It was found that grafting amino-rich PEI chains produced a noticeable increment in positive charge of the PDA/PEI-modified support layer. The isoelectric point of laccase is 3.5-4.0, hence laccase exhibits negative charge at its optimal pH=5. Therefore, the high positive charge of the PDA/PEI-modified support layer at pH 5 can provide a strong electrostatic adsorption to facilitate enzyme capture. For the Zn-modified support layer, the positive charge reduced compared with the PDA/PEI-modified one due to the consumption of amino groups and the formation of negative charged IDA groups, while laccase can be immobilized by affinity binding with Zinc ions [46]. In addition, after the modification, the membrane pore size distribution became narrower, the average pore size was smaller and the water permeability decreased for the PDA/PEI-modified and Zn-modified NF membranes (Figures 2b and 2c), which confirmed the increase of steric hindrance in the support layers. Such structure variation can further restrain the movement of enzyme in the membrane. Therefore, the confinement strength of the modified membranes to laccase was augmented by increasing the charge, affinity and steric effects. The hydrophilicity of the modified support layers also was significantly enhanced compared to the pristine one, thus improving the microenvironment of the immobilized laccase and avoiding product adsorption/accumulation in the membrane (Figure 2d) [47].

3.2 Properties of biocatalytic membranes

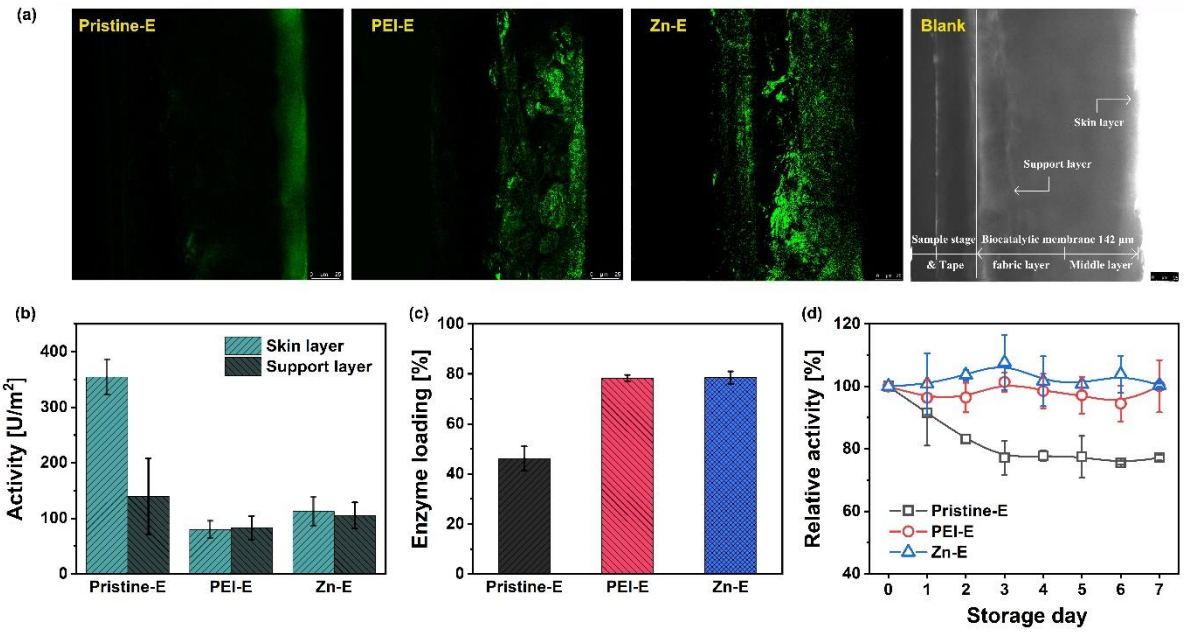

Figure 3. (a) Images of the cross-sections of Pristine-E, PEI-E, and Zn-E by CLSM. Laccase was labelled by FITC and exhibited green emissions. (b) Activity on skin and support layers of Pristine-E, PEI-E, and Zn-E. (c) Enzyme loading of the Pristine-E, PEI-E, and Zn-E. (d) Storage stability analysis by evaluating the relative activity of Pristine-E, PEI-E, and Zn-E over time, where three biocatalytic membranes were soaked in acetic buffer (10mM, pH=5) for 7 days. The error bars represent the standard deviation of at least three measurements.

Figure 3a shows CLSM images of the cross-section of these three biocatalytic membranes. It can be directly seen that laccase in the Pristine-E is stacked beneath the skin layer of the NF membrane while laccase in the PEI-E and Zn-E is uniformly distributed in the whole polysulfone layer of the membrane support. It revealed that the confinement strength of the pristine support layer to laccase was too weak to restrict laccase in the membrane during reverse filtration and all laccase is retained by the skin layer and accumulated beneath it. On the contrary, the modified membranes with increased confinement strength broadened the laccase distribution and alleviated its aggregation. In addition, the modified hierarchical porous structure of the polysulfone layer can immobilize laccase more efficiently due to the high specific surface area and sustained confinement for enzyme. The laccase distribution in the biocatalytic membranes was also evaluated by testing the enzyme activity on the skin and

support layers (Figure 3b). For the Pristine-E, the activity on skin layer was much higher than that on support layer due to a higher local enzyme concentration beneath the skin layer, implying that most of laccase passed through the support layer and accumulated beneath the skin layer. For the PEI-E and Zn-E, the enzyme activities on skin and support layers were almost the same indicating more uniform laccase distribution within the NF membrane. Besides the lower enzyme amount beneath the skin layer, the modification of the support layer inevitably enhanced the steric hindrance of the membrane and reduced the mobility of the enzyme, thereby the activities of the PEI-E and the Zn-E on both skin and support layers were lower than that of the Pristine-E.

As observed in Fig. 3c, the PEI-E and Zn-E exhibited much higher enzyme loading than Pristine-E indicating that the enhanced confinement strength of the modified support layers to laccase was of great benefit to keep laccase inside the membrane. Traditionally, enzyme was immobilized on the surface of the modified skin layer of NF membrane in order to promote the contact between substrate and enzyme, but its enzyme loading was much less compared to that in the support layer (Figure S5) because of the smaller space (less specific area).

As shown in Figure 3d, the catalytic activity of the PEI-E and Zn-E exhibited a negligible decrease after soaking in acetic buffer (10 mM, pH=5) for 7 days which revealed an excellent storage stability. However, for the Pristine-E, the activity decreased in the first three days and then reached a stable state. Unlike covalent binding, enzyme immobilization by physical entrapment normally has little deterioration on enzyme conformation [48]. Hence, enzyme activity loss for the Pristine-E in the beginning was mainly caused by enzyme leakage, and then the balance between enzyme leaching and re-adsorption resulted in a stable enzyme activity [27, 30]. Moreover, the specific activity on BPA removal with different biocatalytic memrbanes was also compared and the Pristine-E showed the highest specific activity due to its lower enzyme loading and higher enzyme mobility. Their specific activity might not change

significantly during storage because enzyme leakage was still mainly responsible for the decline in the BPA removal effiiency (Figure S6).

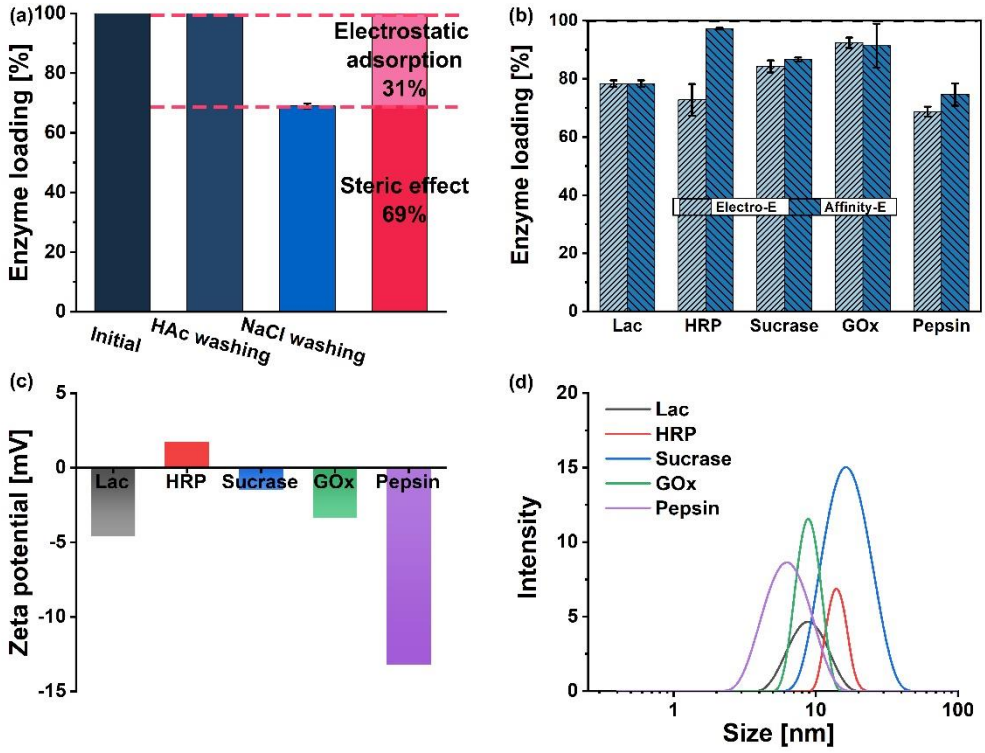

Figure 4. (a) Enzyme loading of the biocatalytic membrane after washing with different solutions; (b) enzyme loading of laccase (Lac), horseradish peroxidase (HRP), sucrase, glucose oxidase (GOx), and pepsin in the PDA/PEI-modified membrane; (c) zeta potential of different enzymes; (d) molecular size of different enzymes. The error bars represent the standard deviation of at least three measurements.

To better understand the enzyme immobilization mechanisms, the PEI-E was washed by acetic buffer (pH 5, 10mM) and NaCl (1 M) respectively until no enzyme was detected in the permeate. The high concentration of salts can shield the electrostatic interaction between laccase and membrane [45]. As shown in Figure 4a, there was no decrease in enzyme loading when the biocatalytic membrane was washed by acetic buffer while 31% of the immobilized laccase leaked after NaCl washing. The results implied that around 31% of laccase might be immobilized by electrostatic adsorption and 79% of laccase was possibly entrapped by steric effect. To demonstrate the versatility of such enzyme immobilization strategy, various enzymes

including glucose oxide (160 kDa), horseradish peroxidase (44 kDa), sucrase (270 kDa), and pepsin (35 kDa) were chosen to be immobilized in the modified NF membrane. These enzymes have both positive and negative electrical charges and different charge density (Figure 4c). Moreover, the size of these enzymes is in the range of 6-17 nm (Figure 4d) and the molecule weight of these enzymes is in the range of 35 to 270 kDa, which cover the size of most of the commonly used enzymes. As shown in Figure 4b, the successful immobilization of these enzymes with high enzyme loading verified its universality.

3.3 BPA removal by biocatalytic membrane

3.3.1 Effect of operational mode

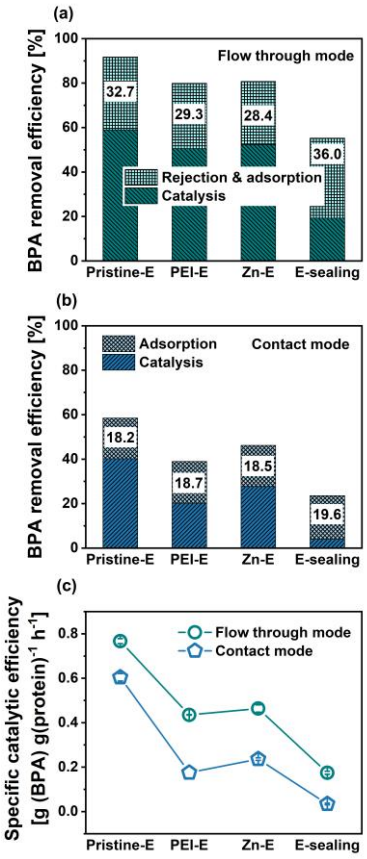

Figure 5. BPA removal efficiency for the pristine-E, PEI-E, Zn-E and E-sealing in flow through mode (a) and contact mode (b). (c) Specific catalytic efficiency of the pristine-E, PEI-E, Zn-E and E-sealing in flow through mode and contact mode. The error bars represent the standard deviation of at least three measurements.

As shown in Figure 5a, BPA removal efficiency of these four biocatalytic membranes when operated in flow through mode was in the order: pristine-E > Zn-E > PEI-E > E-Sealing. The E-sealing showed the highest BPA rejection and adsorption, but the lowest catalytic efficiency and specific catalytic efficiency. The highest BPA rejection and adsorption of the E-sealing were caused by its additional sealing layer which increased the filtration resistance and adsorption capacity to BPA. The lowest catalytic efficiency was due to the inflexible state of the immobilized enzyme and the highest steric hinderance which largely inhibited the laccase activity [27]. In addition, the rejection and adsorption effects for the PEI-E and Zn-E were lower than for the Pristine-E, although the average pore size of the PEI-E and Zn-E was smaller (Figure 2). It may be attributed to the higher hydrophilicity of the modified membranes that lowered the BPA hydrophobic adsorption [49]. Since the modification of the support layer inevitably enhanced the steric hinderance of the membrane and affected the enzyme conformation even without a sealing layer, the specific catalytic efficiency of the PEI-E and Zn-E was lower than that of the Pristine-E, but higher than that of E-sealing (Figure 5c). The specific catalytic efficiency of the Zn-E was a bit higher than that of PEI-E due to its lower confinement strength. The above results indicated that the confinement strength of the membrane to the immobilized enzyme governed its catalytic activity on micropollutant.

As observed in Figures 5a and 5b, the catalytic efficiency of the biocatalytic membranes under flow through mode was much higher than that under contact mode. In static contact mode, the diffusion controlled mass transfer limited the accessibility of BPA to the enzyme and the product removal from the active sites, leading to a poor catalytic efficiency. This problem might be mitigated by employing agitation/membrane vibration or oxygen bubbling in the solution which could increase the shear-induced solute diffusion at the membrane surface as well as introduce oxygen to increase the catalytic activity of laccase. While in flow through mode, the pressure-driven convective transport greatly accelerated the mass transfer of

substrate and product, thereby increasing the catalytic efficiency. The catalytic efficiency of the Pristine-E, PEI-E, Zn-E, and E-Sealing in flow through mode was 1.47, 2.50, 1.89, and 4.87 times of those in contact mode, respectively. Therefore, the flow-through operation produced more promotions to the biocatalytic membranes with higher steric hinderance, further confirming that pressure-driven convective transport through the membrane could overcome the mass transfer resistance in the membrane.

3.3.2 Reusability of biocatalytic membrane

As seen in Figure 6, the PEI-E and Zn-E maintained a long-term stability for BPA removal after 7 reuse cycles in pressure-driven flow through mode. Conversely, the BPA removal efficiency of the pristine-E and E-sealing decreased significantly with reuse cycle. This was attributed to the suitable confinement strength and the higher hydrophilicity of the PDA/PEI-modified and Zn-modified membranes, thereby reducing enzyme leakage, stabilizing enzyme structure, and preventing product accumulation. For the Pristine-E, the decline in BPA removal was mainly caused by the enzyme leakage due to the low confinement strength of laccase in the membrane. For the E-sealing, the unstable BPA removal performance was due to the existence of the sealing layer and the resultant product accumulation that inhibited laccase activity [27]. Therefore, rationally tuning the confinement strength of the membrane to keep a low mass transfer resistance around the immobilized enzyme could delay enzyme leakage and prevent production inhibition, thereby efficiently improving the reusability of the biocatalytic membrane.

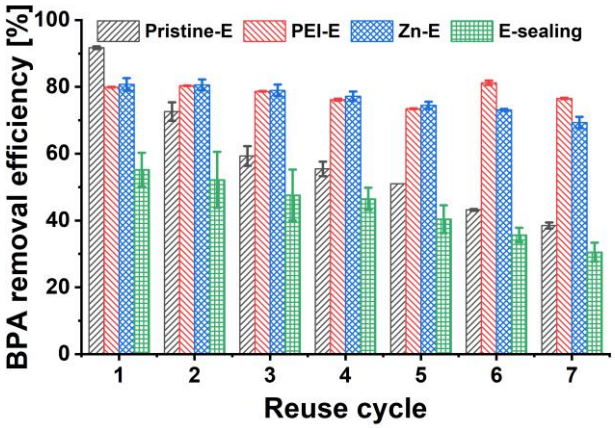

Figure 6. BPA removal efficiency for the Pristine-E, PEI-E, Zn-E and E-sealing over 7 reuse cycles. Operation conditions: the biocatalytic membranes were operated at a permeate flux of 7.46 L m^{-2} h^{-1} for 3h for each batch, 33 mL BPA solution (10mg mL^{-1}) was treated at room temperature (25℃). The error bars represent the standard deviation of at least three measurements.

3.3.3 Continuous operation

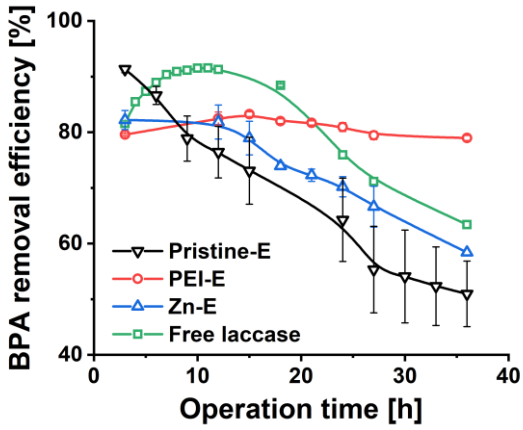

Figure 7. BPA removal by NF membranes with free and immobilized laccase in continuous operations for 36 h. The permeate flux was controlled at 7.46 L m^{-2} h^{-1}. BPA solution (10 mg mL^{-1}) was treated at room temperature (25℃). The error bars represent the standard deviation of at least three measurements.

For continuous operation (Figure 7), the PEI-E exhibited an excellent long-term stability and removed BPA over 36 h with no decline. Unexpectedly, the Zn-E only maintained stable for around 12h and then decreased linearly, reveling that a certain amount of laccase began to

leak from the membrane after 12h. For the Pristine-E, the BPA removal efficiency has been decreasing due to the fast enzyme leakage. For the enzymatic membrane reactor with free enzyme, a climax of the BPA removal efficiency after around 10 h followed by a sharp decline due to enzyme inactivation was observed, clearly revealing that free laccase has the highest activity but lowest stability. Compare with other laccase-based biocatalytic membranes reported in the recent literature, the PEI-E exhibited great advantages in BPA removal efficiency and long-term stability (Table 2).

Table 2. Comparison of the laccase-based biocatalytic membranes for BPA removal

Biocatalytic membranes [a]	Initial BPA concentration (mg L^{-1})	Treat volume (mL)	Operation time each cycle (h)	BPA removal efficiency in the first cycle (%)	Reuse cycle	Final BPA removal efficiency in the last cycle (%)	Throughput (L m^{-2} h^{-1})	Average decline per cycle (%)	Ref
TiO_2 (sol-gel)-PVDF (MF)	34.24	40	24	92	4	84	1.98	2.00	[22]
Cu-IDA-PEI-PVDF (MF)	10	8.8	6	99	5	57	10	8.40	[20]
PDA-NF270 (NF)	10	40	5	88	7	34	5.97	7.70	[26]
Cu-PDA-NF270 (NF)	2	20	6	87	9	77	2.49	1.11	[30]
PAN-MIL-101 (UF)	10	40	5	92	7	62	6.45	4.29	[31]
GO/PDA-NF270 (NF)	10	30	3	67	4	37	7.46	7.50	[27]
$Lac_{4.0}$-HPEI/PES (UF)	0.1	35	4	77	4	73	7.07	1.00	[50]
PEI-E (NF)	10	30	3	80	7	77	7.46	0.43	This work

a MF, microfiltration; UF, ultrafiltration; NF, nanofiltration.

3.4 Mechanism discussion

3.4.1 Motion of the immobilized laccase

Enzymes in living cells are highly dynamic but at the same time rationally confined to enhance the efficiency of metabolic pathways [51]. Therefore, the commodious

microenvironment for maintaining enzyme necessary mobility is an important aspect for efficient catalysis [52]. The motion of the confined laccase in the PEI-E was directly observed by CLSM when the PEI-E was washed under reverse and normal modes respectively (Figure 8a), indicating that the confined enzyme has a certain level of mobility. Furthermore, as illustrated in Figure 8b, the ratio of enzyme activity on skin and support layers fluctuated during the successive washing of the PEI-E and Zn-E in reverse, then normal and again reverse modes, revealing the movement of laccase toward or away from the skin layer. It also showed that the movement of laccase was reversible and controllable. The mobility of the Zn-E was higher than the PEI-E demonstrating that the confinement strength in the Zn-E was lower (Figure 8c), and this also explained why the Zn-E showed a bit higher specific catalytic efficiency (Figure 5c) but worse operating stability (Figure 7) than the PEI-E.

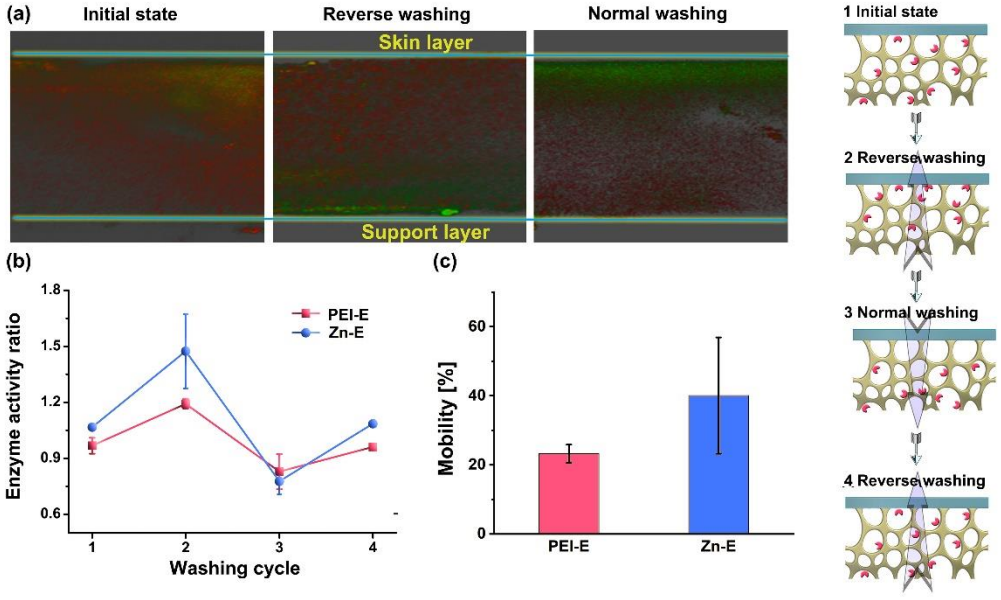

Figure 8. (a) CLSM images of the cross-sections of the PEI-E in initial state, after reverse washing, and after normal washing respectively. The support layer was label with FITC (green emission) and laccase was labeled with rhodamine b (Rhb, red emission). (b) Variation of ratios of enzyme activity on skin and support layers during three washing cycles of PEI-E and Zn-E. (c) Mobility of PEI-E and Zn-E. The picture on the right is the schematic diagram of the movement state of the enzyme under different washing conditions. Conditions: the biocatalytic membranes were washed with acetic buffer (pH 5) at a permeate flux of 45.66 L m^{-2} h^{-1}. The error bars represent the standard deviation of at least three measurements.

3.4.2 Effect of confinement strength on enzyme motion and performance

According to the above discussion, higher confinement strength of the NF membrane can retard enzyme leakage but reduce enzyme catalytic efficiency. In order to further clarify the effect of spatial confinement strength on enzyme motion and performance as well as to find a balance between enzyme activity and stability in the membranes, the biocatalytic membranes with different confinement strength were prepared by changing the PEI grafting time which was set at 0.1, 0.5, 2, 3, and 4 h respectively. The obtained membranes were termed as 0.1PEI-E, 0.5PEI-E, 2PEI-E, 3PEI-E and 4PEI-E. Then a novel parameter, enzyme mobility, was proposed to quantitively reflect the confinement strength of membrane to laccase which was described in Section 2.7.

As depicted in Figures S7 and S8, the increase in PEI grafting time led to a reduction in membrane permeability and an increase in surface positive charge, which enhanced the charge and steric effects of the membrane on laccase, corresponding to a higher confinement strength. Therefore, enzyme loading increased rapidly when the PEI grafting time was prolonged from 0.1 to 2 h, and then reached a plateau with further increasing grafting time (Figure 9a). The specific catalytic efficiency decreased fast with the rapid increase of the enzyme loading, which has been already observed and called enzyme crowding phenomena, that is, higher enzyme loading might induce higher steric hinderance [11]. Therefore, 4PEI-E had the highest confinement strength to the immobilized laccase. The mobility for 0.5PEI-E, 2PEI-E, and 4PEI-E were then tested and shown in Figure 9b. It can be found that the mobility of laccase decreased rapidly with increasing PEI grafting time. This result agreed well with the above findings, indicating that the enzyme mobility could be used to quantify the confinement strength to the immobilized enzyme in the biocatalytic membranes.

Furthermore, as seen in Figure 9c, the specific catalytic efficiency of the biocatalytic membranes increased linearly with the mobility of the immobilized laccase. While the stability of these biocatalytic membranes for BPA removal in the continuous operations became worse at shorter PEI grafting time (i.e. higher enzyme mobility), especially for the 0.1PEI-E and 0.5 PEI-E (Figure 9d). Therefore, it can be concluded that higher enzyme mobility kept enzyme configuration and high activity on BPA removal, but was detrimental to immobilize and stabilize enzyme in the support layer, leading to enzyme leakage during continuous operations. On the other hand, all the biocatalytic membranes with different enzyme mobility and specific catalytic efficiency showed similar BPA removal at the first three hours (Figure 9d), which was explained by a fact that lower enzyme mobility (i.e. less specific catalytic efficiency for BPA removal) normally brought a higher enzyme loading in the membranes. Accordingly, by rationally designing the interior structure and chemical properties of the support layer of the NF membrane, a suitable confinement strength to enzyme can be constructed to obtain an optimal enzyme mobility, thus resulting in both high BPA removal efficiency and stability. Furthermore, enzyme mobility in the membranes may also be used to predict the performance of the biocatalytic membranes.

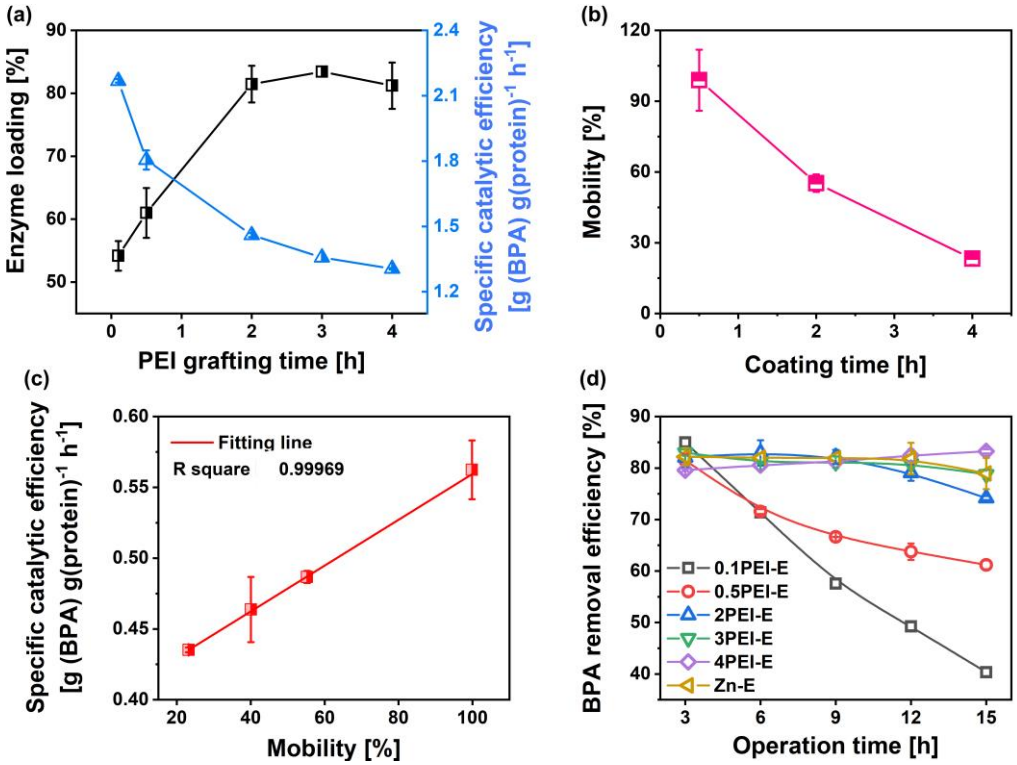

Figure 9. (a) Changes in enzyme loading and specific catalytic efficiency of biocatalytic membranes when PEI grafting time increased from 0.1 to 4 h. (b) Laccase mobility in 0.5PEI-E, 2PEI-E, and 4PEI-E. (c) Relationship between enzyme mobility and specific catalytic efficiency of biocatalytic membranes. (d) BPA removal efficiency of 0.1PEI-E, 0.5PEI-E, 2PEI-E, 3PEI-E and 4PEI-E in continuous operations for 15 h. The permeate flux was controlled at 7.46 L m^{-2} h^{-1}. BPA solution (10 mg mL^{-1}) was treated at room temperature (25°C). The error bars represent the standard deviation of at least three measurements.

It is worth mentioning that although the low mobility of laccase in the modified NF membrane produced a relatively long stability of the biocatalytic membrane, laccase would eventually leak from the support layer of the membrane after a period of flow-through operation in normal filtration mode. Thus, a timely backflushing operation is required to redistribute laccase in the membrane and avoid enzyme leakage (Figure 8a). Consequently, a long-term operating stability of the biocatalytic membrane can be achieved by optimizing enzyme mobility in the membrane and applying periodic backflushing.

3.5 Protein storage and controllable sustained-release device

As mentioned previously, the PDA/PEI-modified and Zn-modified membranes were versatile for immobilizing different enzymes and exhibited excellent storage stability. Accordingly, by controlling the motion of the confined enzymes, such biocatalytic membrane can also be used for protein storage and controllable sustained-release device for reaction and dosing. As shown in Figure 10, laccase in 2PEI-E and Zn-E was released linearly over washing time when operated in flow-through mode.

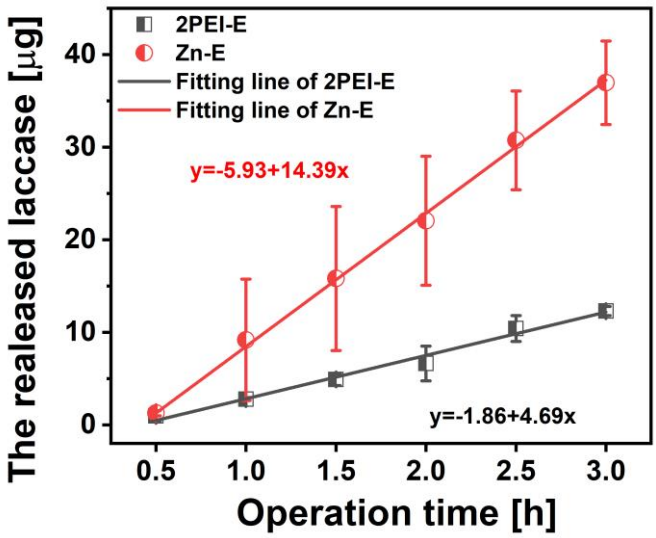

Figure 10. Enzyme controllable sustained-release test. Laccase in the 2PEI-E and Zn-E was released linearly over washing time when the biocatalytic membranes were washed with acetic buffer (10 mM, pH 5) at a permeate flux of 45.66 L m^{-2} h^{-1}. The error bars represent the standard deviation of at least three measurements.

Besides, the prepared biocatalytic membranes can also be used for biosensor, enzymatic biofuel cell, and dyes removal. As we all known, laccase is usually immobilized on the electrodes and used to construct an electrochemical biosensor for the detection of phenol compounds. Moreover, laccase is used to fabricate the enzymatic biofuel cells where phenol compounds are used as fuels. However, some toxins would disturb the electric signals and inactivate the immobilized enzyme, thereby deteriorating the sensitivity and stability of biosensor and biofuel cells. This biocatalytic membrane possesses both separation and

electrocatalytic functions with high enzyme activity and stability. Unfavourable components can be removed by the NF membrane, thus maintaining the sensitivity and stability of the biosensor and the biofuel cells. For dyes removal, most dyes would be retained by the NF membrane, then the residual dyes with small molecular weight that enter the membrane would be degraded by the immobilized laccase, thereby improving dyes removal efficiency.

4 Conclusion

This work demonstrated that laccase could be stabilized in the 3D modified support layer of the NF membrane with a uniform distribution, high enzyme loading, and ultra-high storage stability. Moreover, the modified NF membrane was versatile for different enzyme immobilization. Importantly, this mussel-inspired 3D modification strategy enhanced the confinement strength of the membrane to enzyme with little increment in mass transfer resistance for substrate and products, which effectively delayed the enzyme leakage and at the same time endowed enzyme with a level of mobility for efficient catalysis. Accordingly, the PEI-E exhibited high catalytic activity and long-term stability in both 7 reuse cycles and 36 h continuous operation for micropollutant removal. In addition, the specific catalytic efficiency of the biocatalytic membrane was greatly promoted in flow through mode due to the intensified mass transfer compared with that in contact mode. We also proposed a simple protocol to quantify the mobility of the immobilized enzyme, which could precisely reflect the confinement strength of the modified membranes, as well as the catalytic performance of the biocatalytic membranes. Moreover, the modified membrane was expected to be served as an enzyme storage and controllable sustained-release device for reaction and dosing. This work not only offers a versatile platform to immobilize various enzymes and prepare superior biocatalytic membrane, but also provides guidance to design an optimal confinement environment for enzymes in the membrane, facilitating potential applications of biocatalytic membrane in enhanced bioconversion, drug delivery, and biosensors at small scale.

Acknowledgements

This work was supported by the National Natural Science Foundation of China (No. 21878306) and the Beijing Natural Science Foundation (2192053).

References

[1] M.O. Barbosa, N.F.F. Moreira, A.R. Ribeiro, M.F.R. Pereira, A.M.T. Silva, Occurrence and removal of organic micropollutants: An overview of the watch list of EU Decision 2015/495, Water Res. 94 (2016) 257-279.

[2] J. Qiao, Y. Guo, H. Dong, X. Guan, G. Zhou, Y. Sun, Activated peroxydisulfate by sulfidated zero-valent iron for enhanced organic micropollutants removal from water, Chem. Eng. J. 396 (2020) 125301.

[3] O. Vieira, R.S. Ribeiro, M. Pedrosa, A.R. Lado Ribeiro, A.M.T. Silva, Nitrogen-doped reduced graphene oxide – PVDF nanocomposite membrane for persulfate activation and degradation of water organic micropollutants, Chem. Eng. J. (2020) 126117.

[4] L. Gonzalez-Gil, D. Krah, A.-K. Ghattas, M. Carballa, A. Wick, L. Helmholz, J.M. Lema, T.A. Ternes, Biotransformation of organic micropollutants by anaerobic sludge enzymes, Water Res. 152 (2019) 202-214.

[5] R.A. Sheldon, J.M. Woodley, Role of Biocatalysis in Sustainable Chemistry, Chem. Rev. 118 (2018) 801-838.

[6] F. Shakerian, J. Zhao, S.-P. Li, Recent development in the application of immobilized oxidative enzymes for bioremediation of hazardous micropollutants – A review, Chemosphere 239 (2020) 124716.

[7] X. Mu, J. Qiao, L. Qi, P. Dong, H. Ma, Poly(2-vinyl-4,4-dimethylazlactone)-functionalized magnetic nanoparticles as carriers for enzyme immobilization and its application, ACS Appl. Mater. Interfaces 6 (2014) 21346-21354.

[8] J. Guo, L. Yang, Z. Gao, C. Zhao, Y. Mei, Y.-Y. Song, Insight of MOF Environment-Dependent Enzyme Activity via MOFs-in-Nanochannels Configuration, ACS Catal. 10 (2020) 5949-5958.

[9] S. Shin, H.S. Kim, M.I. Kim, J. Lee, H.G. Park, J. Kim, Crowding and confinement effects on enzyme stability in mesoporous silicas, Int. J. Biol. Macromol. 144 (2020) 118-126.

[10] F. Zhou, J. Luo, B. Qi, X. Chen, Y. Wan, Horseradish Peroxidase Immobilized on Multifunctional Hybrid Microspheres for Aflatoxin B1 Removal: Will Enzymatic Reaction be Enhanced by Adsorption?, Ind. Eng. Chem. Res. (2019).

[11] P. Jochems, Y. Satyawali, L. Diels, W. Dejonghe, Enzyme immobilization on/in polymeric membranes: status, challenges and perspectives in biocatalytic membrane reactors (BMRs), Green. Chem. 13 (2011) 1609.

[12] J. Zdarta, A.S. Meyer, T. Jesionowski, M. Pinelo, Multi-faceted strategy based on enzyme immobilization with reactant adsorption and membrane technology for biocatalytic removal of pollutants: A critical review, Biotechnol. Adv. 37 (2019) 107401.

[13] H. Zhang, Q. He, J. Luo, Y. Wan, S.B. Darling, Sharpening Nanofiltration: Strategies for Enhanced Membrane Selectivity, ACS Appl. Mater. Interfaces (2020).

[14] N. Dizge, R. Epsztein, W. Cheng, C.J. Porter, M. Elimelech, Biocatalytic and salt selective multilayer polyelectrolyte nanofiltration membrane, J. Membr. Sci. 549 (2018) 357-365.

[15] R. Xu, J. Cui, R. Tang, F. Li, B. Zhang, Removal of 2,4,6-trichlorophenol by laccase immobilized on nano-copper incorporated electrospun fibrous membrane-high efficiency, stability and reusability, Chem. Eng. J. 326 (2017) 647-655.

[16] G. Vitola, R. Mazzei, T. Poerio, E. Porzio, G. Manco, I. Perrotta, F. Militano, L. Giorno, Biocatalytic membrane reactor development for organophosphates degradation, J. Hazard. Mater. 365 (2019) 789-795.

[17] J. Luo, S. Song, H. Zhang, H. Zhang, J. Zhang, Y. Wan, Biocatalytic membrane: Go far beyond enzyme immobilization, Eng. Life Sci. (2020).

[18] A.Y. Gebreyohannes, M. Dharmjeet, T. Swusten, M. Mertens, J. Verspreet, T. Verbiest, C.M. Courtin, I.F.J. Vankelecom, Simultaneous glucose production from cellulose and fouling

reduction using a magnetic responsive membrane reactor with superparamagnetic nanoparticles carrying cellulolytic enzymes, Bioresour. Technol. 263 (2018) 532-540.

[19] F.H. Ismail, F. Marpani, N.H. Othman, N.R. Nik Him, Simultaneous separation and biocatalytic conversion of formaldehyde to methanol in enzymatic membrane reactor, Chem. Eng. Commun. (2019) 1-10.

[20] J. Fan, J. Luo, Y. Wan, Aquatic micro-pollutants removal with a biocatalytic membrane prepared by metal chelating affinity membrane chromatography, Chem. Eng. J. 327 (2017) 1011-1020.

[21] Z. Zhu, Z. Chen, X. Luo, W. Zhang, S. Meng, Gravity-driven biomimetic membrane (GDBM): An ecological water treatment technology for water purification in the open natural water system, Chem. Eng. J. 399 (2020) 125650.

[22] J. Hou, G. Dong, Y. Ye, V. Chen, Enzymatic degradation of bisphenol-A with immobilized laccase on TiO2 sol–gel coated PVDF membrane, J. Membr. Sci. 469 (2014) 19-30.

[23] H. Zhang, J. Luo, S. Li, Y. Wei, Y. Wan, Biocatalytic Membrane Based on Polydopamine Coating: A Platform for Studying Immobilization Mechanisms, Langmuir 34 (2018) 2585-2594.

[24] S. Li, J. Luo, Y. Wan, Regenerable biocatalytic nanofiltration membrane for aquatic micropollutants removal, J. Membr. Sci. (2018) 120-128.

[25] H. Zhang, H. Zhang, J. Luo, Y. Wan, Enzymatic Cascade Catalysis in a Nanofiltration Membrane: Engineering the Microenvironment by Synergism of Separation and Reaction, ACS Appl. Mater. Interfaces 11 (2019) 22419-22428.

[26] X. Cao, J. Luo, J.M. Woodley, Y. Wan, Bioinspired Multifunctional Membrane for Aquatic Micropollutants Removal, ACS Appl. Mater. Interfaces 8 (2016) 30511-30522.

[27] H. Zhang, J. Luo, S. Li, J.M. Woodley, Y. Wan, Can graphene oxide improve the performance of biocatalytic membrane?, Chem. Eng. J. 359 (2019) 982-993.

[28] J. Luo, A.S. Meyer, R.V. Mateiu, D. Kalyani, M. Pinelo, Functionalization of a Membrane Sublayer Using Reverse Filtration of Enzymes and Dopamine Coating, ACS Appl. Mater. Interfaces 6 (2014) 22894-22904.

[29] J. Luo, A.S. Meyer, G. Jonsson, M. Pinelo, Enzyme immobilization by fouling in ultrafiltration membranes: Impact of membrane configuration and type on flux behavior and biocatalytic conversion efficacy, Biochem. Eng. J. 83 (2014) 79-89.

[30] X. Cao, J. Luo, J.M. Woodley, Y. Wan, Mussel-inspired co-deposition to enhance bisphenol A removal in a bifacial enzymatic membrane reactor, Chem. Eng. J. 336 (2018) 315-324.

[31] Z. Ren, J. Luo, Y. Wan, Highly Permeable Biocatalytic Membrane Prepared by 3D Modification: Metal-Organic Frameworks Ameliorate Its Stability for Micropollutants Removal, Chem. Eng. J. 348 (2018) 389-398.

[32] S.J. Singer, G.L. Nicolson, The Fluid Mosaic Model of the Structure of Cell Membranes, Science 175 (1972) 720.

[33] M. Schindler, D.E. Koppel, M.P. Sheetz, Modulation of membrane protein lateral mobility by polyphosphates and polyamines, Proc.Natl. Acad. Sci. USA 77 (1980) 1457.

[34] X. Qiu, Y. Wang, Y. Xue, W. Li, Y. Hu, Laccase immobilized on magnetic nanoparticles modified by amino-functionalized ionic liquid via dialdehyde starch for phenolic compounds biodegradation, Chem. Eng. J. 391 (2020) 123564.

[35] R. Tang, Y. Du, L. Fan, Dialdehyde starch-crosslinked chitosan films and their antimicrobial effects, Journal of Polymer ence Part B: Polymer Physics 41 (2003) 993-997.

[36] I.L. Valuev, L.V. Vanchugova, L.I. Valuev, Conformation of Polymer-Carrier Macromolecules and the Activity of Immobilized Enzyme, Appl. Biochem. Microbiol. 56 (2020) 29-31.

[37] M. Jager, S. Schubert, S. Ochrimenko, D. Fischer, U.S. Schubert, Branched and linear poly(ethylene imine)-based conjugates: synthetic modification, characterization, and application, Chem. Soc. Rev. 41 (2012) 4755-4767.

[38] Y. Zhang, M. Barboiu, O. Ramström, J. Chen, Surface-Directed Selection of Dynamic Constitutional Frameworks as an Optimized Microenvironment for Controlled Enzyme Activation, ACS Catal. 10 (2020) 1423-1427.

[39] N.A. Daronch, M. Kelbert, C.S. Pereira, P.H.H. de Araújo, D. de Oliveira, Elucidating the choice for a precise matrix for laccase immobilization: A review, Chem. Eng. J. 397 (2020) 125506.

[40] J.B. Costa, M.J. Lima, M.J. Sampaio, M.C. Neves, J.L. Faria, S. Morales-Torres, A.P.M. Tavares, C.G. Silva, Enhanced biocatalytic sustainability of laccase by immobilization on functionalized carbon nanotubes/polysulfone membranes, Chem. Eng. J. 355 (2019) 974-985.

[41] H.-C. Yang, R.Z. Waldman, M.-B. Wu, J. Hou, L. Chen, S.B. Darling, Z.-K. Xu, Dopamine: Just the Right Medicine for Membranes, Adv. Funct. Mater. 28 (2018) 1705327.

[42] M. Wagner, A.C. Rinkenauer, A. Schallon, U.S. Schubert, Opposites attract: influence of the molar mass of branched poly(ethylene imine) on biophysical characteristics of siRNA-based polyplexese, Rsc Adv. 3 (2013) 12774.

[43] S. Li, J. Luo, X. Hang, S. Zhao, Y. Wan, Removal of polycyclic aromatic hydrocarbons by nanofiltration membranes: Rejection and fouling mechanisms, J. Membr. Sci. 582 (2019) 264-273.

[44] N. Carlsson, A. Borde, S. Wölfel, B. Kerman, A. Larsson, Quantification of protein concentration by the Bradford method in the presence of pharmaceutical polymers, Anal. Biochem. 411 (2011) 116-121.

[45] B.V. Bhut, S.M. Husson, Dramatic performance improvement of weak anion-exchange membranes for chromatographic bioseparations, J. Membr. Sci. 337 (2009) 215-223.

[46] Y. Li, T.S. Chung, S.Y. Chan, High-affinity sulfonated materials with transition metal counterions for enhanced protein separation in dual-layer hollow fiber membrane chromatography, J. Chromatogr. A 1187 (2008) 285-288.

[47] X. Liu, Y. Fang, X. Yang, Y. Li, C. Wang, Electrospun nanofibrous membranes containing epoxy groups and hydrophilic polyethylene oxide chain for highly active and stable covalent immobilization of lipase, Chem. Eng. J. 336 (2018) 456-464.

[48] Y.K. Cen, Y.X. Liu, Y.P. Xue, Y.G. Zheng, Immobilization of Enzymes in/on Membranes and their Applications, Adv. Synth. Catal. 361 (2019) 5500-5515.

[49] C. Ji, J. Hou, K. Wang, Y.H. Ng, V. Chen, Single-Enzyme Biofuel Cells, Angew. Chem. Int. Ed. 56 (2017) 9762-9766.

[50] L.E. Koloti, N.P. Gule, O.A. Arotiba, S.P. Malinga, Recent Applications of Laccase Modified Membranes in the Removal of Bisphenol A and Other Organic Pollutants, International Conference on Pure and Applied Chemistry, 2018.

[51] Z. Zhao, J. Fu, S. Dhakal, A. Johnson-Buck, M. Liu, T. Zhang, N.W. Woodbury, Y. Liu, N.G. Walter, H. Yan, Nanocaged enzymes with enhanced catalytic activity and increased stability against protease digestion, Nat. Commun. 7 (2016) 10619.

[52] X. Li, Y. Xu, K. Goh, T.H. Chong, R. Wang, Layer-by-layer assembly based low pressure biocatalytic nanofiltration membranes for micropollutants removal, J. Membr. Sci. 615 (2020) 118514.